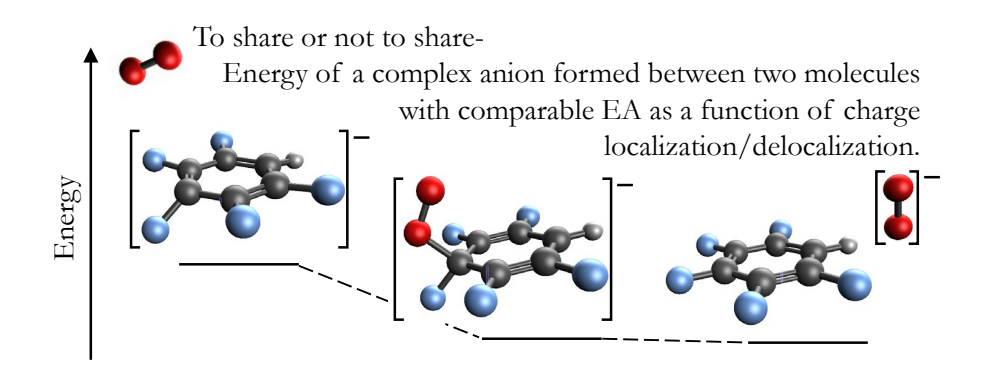
Graphical Abstract

Charge distribution in oxygen-fluorobenzene complex anions $[\mathbf{O}_2 \cdot \mathbf{C}_6 \mathbf{H}_{6-n} \mathbf{F}_n]^-$ (n = 0 - 6).

Jeremy U. Davis, Caroline Chick Jarrold, Thomas Sommerfeld



Highlights

Charge distribution in oxygen-fluorobenzene complex anions $[\mathbf{O}_2 \cdot \mathbf{C}_6 \mathbf{H}_{6-n} \mathbf{F}_n]^ (n=0-6)$.
Jeremy U. Davis, Caroline Chick Jarrold, Thomas Sommerfeld
 Photodetachment probes charge-transfer excitations in anion-molecule complexes
 O₂⁻ and flurorinated benzenes form strongly bound anion-molecule complexes
 Possible binding motifs: non-conventional hydrogen bonds and C-O contacts
 Hydrogen bonded complexes show little anion to molecule charge donation
C-O bonded complexes show substantial anion to molecule charge donation

Charge distribution in oxygen·fluorobenzene complex anions $[O_2 \cdot C_6 H_{6-n} F_n]^-$ (n = 0 - 6).

Jeremy U. Davis^a, Caroline Chick Jarrold^{b,*}, Thomas Sommerfeld^{a,**}

^aDepartment of Chemistry and Physics, Southeastern Louisiana University, SLU 10878, Hammond, LA, 70402, USA
^bDepartment of Chemistry, Indiana University, Bloomington, Indiana, 47405, USA

Abstract

Recently, temporary anion states of fluorine substituted benzenes have been probed via photodetachment experiments on oxygen-fluorobenzene anion complexes $[O_2 \cdot C_6 H_{6-n} F_n]^-$, n=0...6. Here, we complement these experiments with a computational characterization. For the ground electronic states, two isomers are identified: The first isomer class shows non-conventional hydrogen bonds, while the second shows carbon-oxygen contacts. For both isomer classes, the electron affinity of the complex is significantly higher than that of either moiety, and the electron affinity increase upon complex formation is studied in detail. Both isomer classes show strong O_2^- – $C_6H_{6-n}F_n$ interactions, and the extent of charge donation from O_2^- to the organic moiety is characterized. Moreover, we characterize charge-transfer excited states of $[O_2 \cdot C_6H_{6-n}F_n]^-$ anion complexes corresponding to neutral O_2 bound to $C_6H_{6-n}F_n^-$. The charge transfer complexes form doublets and quartets, and here we focus on the minimal energy structure of the quartet state and characterize the doublet at the same geometry.

Keywords:

keyword atomic and molecular structure, chemical binding, electronic structure of atoms & molecules, electron correlation calculations for atoms & ions, density functional calculations

2000 MSC: 81V19, 81V99

1. Introduction

Anion photodetachment experiments probe both direct and resonant detachment of an excess electron, where resonant detachment proceeds by excitation into the empty levels of the anion followed by autodetachment of the excess electron. In both cases, the bound ground state of an anion is laser-excited into a continuum state, and the kinetic energy of the detached electron is measured. A striking difference between the two processes lies in the longer lifetimes of resonance states.

Whether photodetachment spectra of molecular anions are broad or sharp is affected by two factors: First, if the anion and neutral possess significantly different equilibrium structures, the energy of the absorbed photon is split in multiple ways between the outgoing electron and the final internal energy of the neutral molecular system, leading to broad spectra. In contrast, detachment from dipole-bound anions yield very narrow electron kinetic energy distributions, because the geometries of these states align almost perfectly with the respective neutral leading to very large Franck-Condon factors for the zero-zero vibrational transition.[1, 2, 3]

The second factor is lifetime broadening due to the short lifetime of the continuum state. Direct detachment transitions, for the reasons described above, can be broad, but resonant photodetachment transitions can be broad, too, because

Email addresses: cjarrold@indiana.edu (Caroline Chick Jarrold), Thomas.Sommerfeld@selu.edu (Thomas Sommerfeld)

many electronic resonances show short lifetimes on a vibrational timescale. However, sharper spectra are possible if the laser-excitation is targeted into a resonance state with a lifetime sufficiently long to reveal vibrational structure.

Many small organic molecules such as benzene, ethylene, or formaldehyde don't form bound anions, and these molecules cannot be studied directly via photodetachment. However, the scope of photodetachment experiments can be extended to this class of molecules by investigating anion-molecule complexes: A stable anion such as I⁻, OH⁻, or O₂ is 'complexed' with the neutral of interest. The anion-molecule complex can then be photodetached, imparting the photoelectron with a kinetic energy that is resonant with a temporary anion state of its neutral partner. Part of the spectrum then corresponds to laser excitation of the bound electron of the anion into empty levels of the neutral that will then autodetach. While photodetachment spectra for anion-molecule complexes are often no more complex than those of bare molecular anions, additional complications can arise if the ground state of the anion-molecule complex shows significant charge transfer because the anion is a strong donor or the neutral molecule is a strong acceptor.[4]

Recently, temporary anion states of various substituted fluorobenzene molecules have been studied via photodetachment spectroscopy of oxygen-fluorobenzene anion complexes $[O_2 \cdot C_6 H_{6-n} F_n]^-$, $n = 0 \dots 6.[5]$ The well-known direct detachment spectrum of O_2^- exhibits broad vibrational progressions of transitions to the ground triplet state and low-lying singlet neutral states of O_2 .[6] Anion-molecule complexes formed between O_2^- and neutral molecules therefore yield more broad-

^{*}Corresponding author

^{**}Corresponding author

ened spectra, as shown in previous studies, owing to the large difference in equilibrium intermolecular distances between the anionic precursor and resulting neutral van der Waals complexes.[7]

In photodetachment experiments on anion-molecule complexes, resonances, or temporary anion states, of the neutral partner become, in general, evident as enhancements of electron signal at kinetic energies coinciding with the temporary anion state. This situation is analogous to electron transmission spectra of neutral molecules; however, the electron beam is replaced by the anion, which serves as a proximal electron source. The temporary anion states of the fluorobenzenes determined in this manner and reported previously [5] were generally in agreement with limited electron transmission spectra of benzene, [8] monofluorobenzene,[9] and difluorobenzene, [10] along with a previously reported computational study.[11] However, there is a fundamental difference between electron transmission spectroscopy and photodetachment of anion-molecule complexes, since the neutral targeted for study is perturbed by the partner anion in the latter case. In this study, we further explore the electronic structures of the valence-bound anions of these complexes. Specifically, we characterize the geometrical structures of $[O_2 \cdot C_6 H_{6-n} F_n]^-$ (n = 0-6) complexes and compare the electron attachment properties as well as the charge distributions in the complexes to that in their building blocks. Moreover, we briefly consider anion states corresponding to charge-transfer from the O_2^- anion to the organic neutral.

2. Computational Methods

In this paper we study $[O_2 \cdot C_6 H_{6-n} F_n]^-$ (n=0-6) anion complexes as well as electron attachment to their sub-units, O_2 and $C_6 H_{6-n} F_n$. The basic properties helpful for interpreting photoelectron spectra are the adiabatic electron affinities (AEA) and vertical detachment energies (VDE). Moreover, we examine the charge distribution in the $[O_2 \cdot C_6 H_{6-n} F_n]^-$ ground states.

2.1. Minimal energy structures

This subsection summarizes the investigation of different methods for geometry optimization of typical neutral and anionic systems considered in this study. While these findings could be broken up into a methods part and a results part that would be presented in section 3 below, it seems more straightforward to combine both into a single unit (this subsection).

In a first step, minimal energy geometries need to be identified for all $[O_2 \cdot C_6 H_{6-n} F_n]^-$ anions, their associated neutral complexes as well as their anionic and neutral sub-units. This set contains simple neutral molecules, molecular anions as well as molecule clusters and neutral-anion complexes. Owing to the diverse set, it is not so clear which density functional (DF) represents a good compromise between computational cost and reliability.

In the early stages of the project, $C_6H_3F_3$ was chosen as a test subject, because it forms a vertically stable anion as well as two $O_2^- \cdot C_6H_3F_3$ anion complexes displaying different O_2^- binding motifs. For this set of three anions and their

three associate neutral structures, minimal energy structures were computed using orbital-optimized MP2 theory (OOMP2) as well as different DFs: BLYP, B3LYP, PBE, long-rangecorrected PBE, PW6B95, R2Scan, Scan, ωB97X, ωB97X-V, B2GP-PLYP [12, 13, 14, 15, 16, 17, 18, 19, 20, 21, 22]. For all DFs lacking built-in dispersion corrections, explicit corrections (D3 or D3BJ) were included. All geometry optimizations employed the def2-TZVPPD Ahlrichs basis set,[23] and all optimizations were followed by single-point energy evaluations with the domain-based local-pair natural-orbital coupledcluster method with single, double, and non-iterative triple substitutions (DLPNO-CCSD(T)),[24] where tight thresholds were applied for all cutoff parameters (10⁻⁷ for the pair naturalorbital (PNP) occupation number cutoff, 10^{-5} for the estimated pair correlation energy cutoff, $5 \cdot 10^{-3}$ for the PNO domain construction cutoff, and 10^{-3} for a cutoff controlling the local fit (see the manual of the ORCA package [25, 26])). The DLPNO-CCSD(T) energies provide a criterion to judge both the quality of the different geometries and the quality of the predicted electron affinities.

The exploratory calculations did not yield a clearly preferable method. All functionals performed well for a particular subset of systems or properties, however, none performed outstandingly across the board. Our test set is, of course, far too small to evaluate DFs in a meaningful way, but for the particular systems at hand, the following trends emerged: First, B3LYP-D3 normally yields the best geometries for neutral molecules. Many other DFs yield structures that have similar DLPNO-CCSD(T) energies with ω B97X-D3BJ and B2GP-PLYP geometries normally less than 1kJ/mol and at most less than 3kJ/mol above the B3LYP-D3 result. Second, ωB97X-D3BJ in general yields the best geometries for anions, and B2GP-PLYP performs almost equally well. In particular, for the anion complex showing a close oxygen-carbon contact, both ω B97X-D3BJ and B2GP-PLYP perform significantly better than B3LYP-D3 and a variety of other DF methods that overestimate the O-C bond lengths. Third, B2GP-PLYP predicts the most accurate EAs by far. All DF methods investigated overbind the excess electron with respect to DLPNO-CCSD(T), that is, the DF AEAs and VDEs are too high. However, while B3LYP-D3 and ω B97X-D3BJ typically overshoot by values in the 0.1 to 0.2eV range with maximum deviations of almost 0.4eV, the B2GP-PLYP predictions are normally within 0.1eV of the DLPNO-CCSD(T) value and often much closer.

Owing to this mixed performance, we computed three sets of geometries using $\omega B97X\text{-}D3BJ$, B3LYP-D3, and B2GP-PLYP, and it turned out that for other systems these three methods generally agree with each other (differences hardly noticeable in a figure plotting three geometries on top of each other). However, vibrational frequencies and zero-point-energies were computed only with $\omega B97X\text{-}D3BJ$, and some of the more intricate analyses (see below) are done using only the $\omega B97X\text{-}D3BJ$ geometry or only the B2GP-PLYP density.

All geometry optimizations and DLPNO-CCSD(T) single-point energy evaluations have been performed with the ORCA package of programs, version 5.0.[25, 26]

2.2. Electron affinity

At a basic level, the electron affinity EA of a molecular system is characterized by three values: First, the vertical detachment energy (VDE) is the energy difference between neutral and anion evaluated at the geometry of the anion. A positive VDE implies that the anion is at least locally bound, and the VDE is loosely related to the peak of the photo-electron signal through the Franck-Condon principle. Second, the adiabatic electron affinity (AEA) is the same difference, but both neutral and anion energy are evaluated at the respective minimum energy structures, where it is understood that two related minimal energy structures are considered in the sense that adiabatic relaxation of a detached anion would lead to the neutral structure. This energy corresponds in principle to the onset of the photoelectron signal, while the practical onset is impacted by the intensities of the low-energy transitions in comparison with the background level. Alternatively, the AEA can be defined as the difference between the most stable neutral and most stable anion structures, but this definition may lead to unrelated minima and therefore experimentally irrelevant AEA values. Third, the vertical electron affinity (VEA) is again the energy difference between neutral and anion, but this time at the geometry of the neutral.

The VEA of small organic molecules is normally negative, indicating that at the geometry of the neutral, the anion forms an unstable temporary state. In scattering language, the negative VEA corresponds to the resonance position that would be observed in an electron scattering experiment. Negative VEAs can only be computed with special methods such as complex absorbing potentials, Hazi-Taylor stabilization methods, or analytical scaling methods.[27, 28] The fluorobenzene molecules considered here fall into this group, however, their negative VEAs are not directly relevant in the present context, and we don't attempt to compute them accurately. For plotting purposes, we estimate the VEA qualitatively (see below) through semi-empirical scaling of equation-of-motion coupled-cluster VEA values obtained using a compact basis set.[29]

Similarly, a negative VDE indicates that an anion is unstable at its own minimal energy structure, while a positive VDE indicates that it is stable to vertical electron loss. If the former is true, again, special methods are required (see above). If the latter is true, both VDE and AEA can be readily computed with standard electronic structure methods. Anions possessing positive VDEs are at least *locally stable*, that is, electronically stable in the vicinity of their own minimal energy structure.

The most straightforward method to compute electron affinities involves computing the difference of absolute energies. Some care is needed when selecting methods;[30, 31] for example, it has been documented that while DF tends to describe attachment into open shells reliably, results for attachment to closed-shell molecules can be more mixed.[32] Here, DLPNO-CCSD(T) single point energies with the aug-cc-pVTZ[33] are used for most cases. In addition, the VDE and AEA of $C_6H_{6-n}F_n$ (n=3-6) are computed using CCSD(T) as well as the equation-of-motion coupled-cluster methods EOM-CCSD and EOM-CCSD(T)(a)*, where the latter corrects the

EOM-CCSD attachment energy for triple excitations in a manner designed to be compatible to the CCSD(T) triple excitations correction of the ground state.[34] For all coupled cluster and equation-of-motion coupled-cluster calculations beyond DLPNO-CCSD(T), the CFOUR package has been used.[35]

While the discussed electronic structure methods are suitable to compute accurate electron affinities for the molecules and complexes considered, basis sets beyond triple-zeta quality are required for fully converged results. Based on the typical performance of the used methods,[36, 30, 31] the error associated with the triple- ζ basis set can be expected fall into the 0.1 to 0.2 eV region. Reducing the error significantly, is computationally prohibitive for us, since quadruple- ζ or even quintuple- ζ calculations would be required for open-shell non-symmetric complex anions consisting of up to 14 non-hydrogen atoms.

We note that the EOM-CCSD method computes attachment energies *directly*, in other words, VEAs or VDEs are obtained as eigenvalues in a single calculation. As a consequence, an EOM-CCSD VDE has to be combined with the relaxation energy of the neutral to its minimal energy geometry to infer an AEAs. Here we use CCSD(T) relaxation energies—and not CCSD relaxation energies—because in this scheme the AEA is computed as a sum of two unrelated energies, and in order to obtain the most reliable total, the most reliable input data should be used.

After computing VDEs and AEAs, it is possible to correct for vibrational effects. While VDE corrections require a Franck-Condon analysis, the AEA correction is simply the difference in zero-point energies of the neutral and the anion. As anions typically show occupied anti-bonding orbitals, their vibrational modes tend to show lower frequencies than the respective modes of the neutral, and zero-point corrections are normally stabilizing in the sense that the AEA is increased. This trend holds for all considered systems.

2.3. Atomic charges

To answer the question, "Upon complex formation, how much of the negative charge of the O_2^- ion—if any—is donated to the fluorobenzene unit?", we computed atomic charges using the natural population analysis (NPA) as well as the minimal basis iterative Stockholder (MBIS) "atoms-in-molecules" schemes.[37, 38] Both analysis schemes yield similar results. Still, any individual atomic charge should always be taken with a grain of salt. Charge-changes and trends tend to be more meaningful, and we therefore focus on changes in atomic charges upon complex formation and trends in the charge of the O_2 -moiety for different isomers.

To compute atomic charges, $\omega B97X$ -D3BJ single-point calculations were performed with Psi4 [39] version 1.6. Psi4 directly computes MBIS charges and was used to create .molden files, which then served as inputs for the NPA code JANPA.[40]

3. Results and Discussion

The goal of this study is to characterize bound anion states for the members of the series of increasingly fluorinated benzenes studied with photodetachment spectroscopy in Ref. [5]. In Ref. [5], one $C_6H_{6-n}F_n$ isomer was considered for every n=0-6: For n=0,1,5 and 6, only one unique isomer exists, so for these four values of n everything is straightforward. For n=2,3 and 4, three isomers exist, respectively, and for these values of n, only the high-symmetry isomers with vanishing dipole moment were investigated: 1,2-difluorobenzene, 1,3,5-trifluorobenzene, and 1,2,4,5-tetrafluorobenzene. Complex formation with oxygen does not affect the polarity properties of these molecules in any significant way,[5] and therefore all molecules and complexes considered in Ref. [5] show dipoles far below the critical value for possessing dipole bound states. Here, we focus on this set of isomers, too. To avoid repeating clumsy expressions such as 'the seven considered systems,' we refer to this group as *fluorobenzenes* or *organic moieties*.

3.1. $C_6H_{6-n}F_n$ molecules

We start with the VDE and AEA trends for the seven fluorobenzenes. On the one hand, the calculations for the isolated molecules are needed so that trends upon O_2^- complex formation can be established. On the other hand, far more sophisticated electronic structure methods can be used for the bare molecules, which are smaller and have high symmetry. Hence, these systems will be used to calibrate the more approximate methods, which will then be employed to study the O_2^- complexes.

As one would expect, the electron affinity of $C_6H_{6-n}F_n$ molecules (see Tab. 1; the specific values are discussed below) correlates strongly with increasing fluorine substitution, a trend that has been established in Ref. [11] using density functional calculations and a slightly different definition of AEA (see section 2.2). Benzene, mono, and difluorobenzene do not form stable anions and represent, even at the anion geometry, temporary species with negative VDEs. Special techniques are required to compute the energies and lifetimes of these electronic resonances.[27, 28] Tri and tetrafluorobenzene occupy a middle ground in that their anions possess a positive VDE and negative AEA. These two anions can be expected to show substantially longer lifetimes than the less heavily substituted fluorobenzenes; however, their lifetimes are probably still short on a mass spectrometric timescale. Finally, penta and hexafluorobenzene form stable anions.

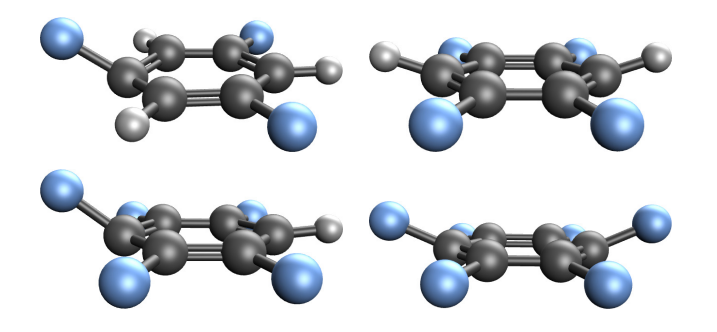


Figure 1: Structures of the four vertically stable fluorobenzene anions $C_6H_{6-n}F_n^-\ (n=3-6).$

Table 1: VDE and AEA in eV of $C_6H_{6-n}F_n^-$ (n=3-6) computed with various coupled-cluster methods and the aug-cc-pVTZ basis set. All coupled-cluster energies were evaluated at $\omega B97X-D3BJ/def2-TZVPPD$ geometries, and the AEA values include zero-point corrections.

	F F			
	method	AEA	VDE	
$C_6H_3F_3$	DLPNO-CCSD(T)	-0.565	0.395	
$C_6H_2F_4$	DLPNO-CCSD(T)	-0.231	0.228	
	CCSD(T)	-0.210	0.237	
	EOM-CCSD	-0.357	0.090	
	EOM-CCSD(T)(a)*	-0.171	0.276	
C_6HF_5	DLPNO-CCSD(T)	0.174	1.252	
	CCSD(T)	0.207	1.262	
	EOM-CCSD	0.462	1.063	
	EOM-CCSD(T)(a)*	0.418	1.292	
C_6F_6	DLPNO-CCSD(T)	0.400	1.395	
	CCSD(T)	0.463	1.435	
	EOM-CCSD	0.546	1.518	
	EOM-CCSD(T)(a)*	0.502	1.474	

Equilibrium geometries of those anions with positive VDEs are shown in Fig. 1. All neutrals are, of course, planar, and all anions show puckering distortions. However, the puckering distortion itself displays an odd/even pattern: For tri and pentafluorobenzene, there is only one major structural change: A single fluorine atom bends out of plane by about 35° and the associated CF bond is stretched by about 0.1 Å, while the other fluorine atoms remain in the plain and their bonds are only modestly elongated (0.04 Å). In other words, the odd n anions show local puckering distortions. In contrast, the anions of tetra and hexafluorobenze deform along normal mode-like puckering coordinates: Four fluorine atoms bend down, while the other two atoms bend up. Since these distortions affect all substituents, the out-of-plane distortions are smaller, and the CF bonds are stretched by only 0.04 Å.

AEA and VDE values computed with different coupled-cluster methods are summarized in Tab. 1, and these values are combined with estimated negative VEAs (see section 2.2) to establish schematic potential energy curves shown in Fig. 2. Regarding the different electronic structure methods, we note that DLPNO-CCSD(T) and CCSD(T) agree well with each other (within 0.07 eV). With the exception of the AEA of pentafluorobenzene, EOM-CCSD(T)(a)* also agrees very closely with CCSD(T) (within 0.05 eV), while EOM-CCSD shows slightly larger discrepancies of up to 0.25 eV, as one would expect for valence states.

While the deviations of the different results in Tab. 1 don't provide a measure of absolute precision, the small discrepancies between DLPNO-CCSD(T) and CCSD(T) suggest that the DLPNO approximation works well for electron affinities. This is far from obvious and shows that the independent DLPNO approximations for the neutral and anion are balanced. Regarding the prediction of AEAs as such, there is substantial experience with CCSD(T), while there is very little experience with EOM-CCSD(T)(a)*. Predicting electron affinities of closed-shell neutrals represents a notoriously challenging task,[32, 31] and we expect most of the error to be associated with the triple- ζ basis

set.[36, 30, 31] Based on the typical performance of the used methods, deviations from the experimental results are likely to fall into the 0.1 to 0.2 eV region.

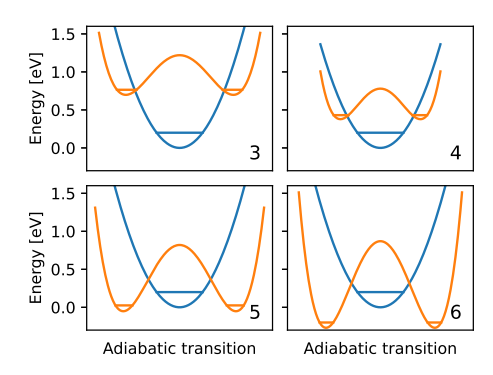


Figure 2: Schematic potential energy curves of the neutral fluorobenzenes $C_6H_{6-n}F_n$ (n=3-6) (blue) and their associated anions (orange). The adiabatic transition coordinate transforms the planar neutral into the respective puckered anion structures (see Fig.1). For n=3 and n=5 this nuclear coordinate corresponds essentially to the localized bend and stretch of a single C–F bond; for n=4 and n=6 it essentially corresponds to ring pucking.

The picture emerging is best represented by the schematic potential curves shown in Fig. 2. The trend to stabilization of the π^* orbital with increasing fluorination is clearly visible. Single occupation of the doubly-degenerate (n=0,3,6) or near doubly-degenerate (n=1,2,4,5) π^* orbital leads to out-of-plane symmetry breaking and puckered structures. Trifluorobenzene forms the first vertically stable anion, and pentafluorobenzene forms the first truly stable anion. Fig. 2 also shows that the difference in zero-point energies is a major stabilizing factor of about 0.13 eV, and this contribution can be expected to be larger if anharmonic corrections are taken into account.

3.2. Low-energy $[O_2 \cdot C_6 H_{6-n} F_n]^-$ complexes

Neutral O_2 and $C_6H_{6-n}F_n$ bimolecular van der Waals complexes show binding energies of a few kJ/mol, and sample at experimental temperatures large regions of nuclear coordinate space because of the flat intermolecular potential. In contrast, the interaction between an O_2^- anion and a $C_6H_{6-n}F_n$ molecule is much stronger: $50-90\,\mathrm{kJ/mol}$ (Tab. 2). The resulting $[O_2\cdot C_6H_{6-n}F_n]^-$ complexes form two well-defined classes of equilibrium structures: structures with $O\cdots H$ contacts (Aisomers) and structures with $O\cdots C$ contacts (B-isomers) (see Fig. 3).

The CH···O interactions present in the A-isomers can be characterized as non-conventional hydrogen bonds.[41] In this particular context, the acceptor oxygen carries a significant negative charge and the resulting bonds are much stronger than typical conventional or non-conventional hydrogen bonds between neutral donor-acceptor pairs. From a bond-length perspective, O···H-bond distances of A-isomers fall in the range of 1.7 to 2.1 Å, which overlaps the length range of typical hydrogen bonds (1.6 to 2.0 Å). We will therefore refer to A-isomers as non-conventional hydrogen-bonded or simply hydrogen-bonded isomers.

Moreover, if both A and B isomers can be formed, the A-isomer is more stable (see below and Tab. 2). For n = 0 - 2, the

 O_2^- anion lies in the ring plane so as to enable a second weaker oxygen-hydrogen contact, while for n = 3 - 5, the O_2^- ion can only interact with a single hydrogen atom and is therefore oriented perpendicular to the ring plane (see Fig. 3 left hand side).

Table 2: Dissociation energies for A and B isomers into O_2^- in the respective organic neutral. All energy differences were computed with the DLPNO-CCSD(T) method and the aug-cc-pVTZ basis set using ω B97X-D3BJ geometries. All energies are in kJ/mol.

n	isomer A	isomer B
0	49.0	_
1	63.1	_
2	72.2	_
3	65.8	53.0
4	83.5	_
5	93.0	85.4
6	_	67.4

In B-isomers, oxygen-carbon interactions are formed. However, for n=0,1,2, and 4, the B-isomer lies much higher in energy than the A-isomer and shows only a shallow minimum with respect to C-O bond dissociation. We don't consider these high-energy species here. For n=3 and 5, the B-isomers have much lower energies, about 13 and 8 kJ/mol above their respective A-isomers (the relative energies of the isomers is identical to the relative dissociation energies in Tab. 2). Reflecting the low relative energy for n=3,5, the carbon-oxygen bond in the B-isomers is short (about 1.6 Å), and the barrier for breaking it is high. For n=6, the B-isomer is, of course, the only complex (see Fig.3 right hand side), but the carbon-oxygen interaction is rather weak, as indicated by the long C-O bond length of 2.0 Å.

B-isomers resemble Meisenheimer intermediates found in nucleophilic aromatic substitution reactions. [42] A Meisenheimer intermediate is formed when a nucleophile binds to a leaving-group substituted aromatic carbon. Subsequently either the original nucleophile or the leaving group may detach, resulting in the reactant or the substituted product. In that sense the n=3,5 B-isomers represent tight Meisenheimer complexes, while the n=6 B-isomer represents a loose Meisenheimer complex.

Table 3: Increase of the AEA of O_2 upon complex formation: $\Delta AEA = AEA([O_2 \cdot C_6H_{6-n}F]_n) - AEA(O_2)$. AEAs have been computed with the DLPNO-CCSD(T) method and the aug-cc-pVTZ basis set using $\omega B97X$ -D3BJ geometries. All energies are in eV.

n	isomer A	isomer B
0	0.45	
1	0.61	
2	0.72	_
3	0.65	0.50
4	0.82	_
5	0.90	0.83
6	_	0.64

Both isomer types show substantially larger AEAs than O_2 itself. We list the AEA changes ΔAEA for all complexes in Tab. 3 because ΔAEA can be written as a chemical reaction

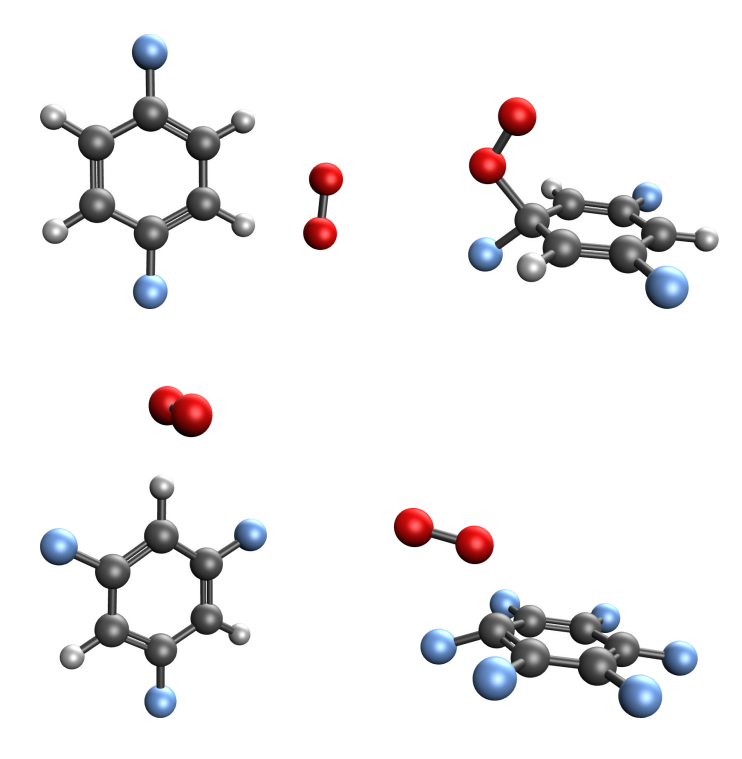


Figure 3: Typical structures of $[O_2 \cdot C_6 H_{6-n} F_n]^-$ anions. Hydrogen-bonded structures (A-isomers) on the left and Meisenheimer-like structures (B-isomers) on the right.

 $O_2^- \cdot C_6 H_{6-n} F_n + O_2 \longrightarrow O_2 \cdot C_6 H_{6-n} F_n + O_2^-$ (n = 3 - 6) that is formerly isodesmic—the number and type of valence bonds remains unchanged—and the predictions for the associated reaction energies are thus expected to be far more reliable than absolute AEA values.

Table 3 reveals several trends: For the first three A-isomers, Δ AEA increases from 0.45 to 0.72 eV as the organic moiety gets more electron deficient, while the O_2^- ion binding motif stays constant (O_2^- interacts with two hydrogen atoms). For the next three A-isomers, the O_2^- ion interacts only with a single hydrogen atom, so Δ AEA decreases in going from n=2 to n=3; however as the fluorobenzene unit increases further in electron deficiency, Δ AEA continues to grow accordingly (Tab. 3). For the two related B-isomers (n=3 and 5), the trend is similar: Δ AEA grows with the electron deficiency of the aromatic ring. The case of hexaflurobenzene is unique as it represents the only loose B-isomer, and according to the weaker anion-neutral interaction, its AEA changes less than the AEA of the B-isomer of $[O_2 \cdot C_6 HF_5]^-$.

3.3. Charge distribution in $[O_2 \cdot C_6 H_{6-n} F_n]^-$ complexes

Having discussed the structures and electron acceptor properties of both the increasingly substituted fluorobenzene units as well as of the resulting $[O_2 \cdot C_6 H_{6-n} F_n]^-$ complexes, let us now turn to the question of how much of the negative charge of the O_2^- ion is donated to the benzene derivative upon complex formation.

An indirect measure of the O_2^- to aromatic system charge donation is the predicted change of the O_2^- bond length upon com-

plex formation. Using the B2GP-PLYP DF, O_2 and O_2^- are predicted to show bond lengths of 1.208 and 1.345 Å, close to the well-known experimental results. The more electron density is donated, the more the predicted bond length will decrease.

Table 4 shows O_2 bond length changes for all $[O_2 \cdot C_6 H_{6-n} F_n]^-$ complexes. The changes are small—less than 0.05 Å or 35% of the bond length difference between O_2^- and O_2 —and one may rightly ask whether changes in this order of magnitude are meaningful. However, the changes is not expected to be large: The O_2^- bond is a strong covalent bond, and formation of a complex cannot have a pronounced impact on its length. Second, the value for the change is a difference, in other words, it benefits from error compensation in the computation for reactants and products, and is expected to be far more reliable than the absolute bond lengths themselves. Last, the computed changes fall into three groups, less than 1%, 5-6%, and 27-35%, and the trend regarding these groups is certainly reliable.

Table 4: Charge distribution in $[O_2 \cdot C_6 H_{6-n} F_n]^-$ (n=3-6). The second and third columns list the decrease in the O-O bond-length $(\Delta(O-O))$ upon complex formation: $O_2^- + C_6 H_{6-n} F_n \longrightarrow [O_2 \cdot C_6 H_{6-n} F_n]^-$ (n=3-6) in % of the bond difference between neutral O_2 and the O_2^- anion of 0.137 Å. All minimal energy structures for this comparison were computed with the B2GP-PLYP DF. The forth and fifth column list total NPA-based charges on the " O_2^- " moiety $(\mathcal{Q}(O_2))$ in the respective complex anions computed as the sum of the two oxygen atom charges. For the NPA, the ω B97X-D3BJ density was analyzed.

$\Delta(O - O)$		$Q(\mathrm{O}_2)$		
n	A	В	A	В
0	0.4	_	-0.953	_
1	0.4	_	-0.948	_
2	0.6	_	-0.937	_
3	4.4	35.0	-0.904	-0.399
4	6.1	_	-0.883	_
5	6.2	34.0	-0.875	-0.385
6	_	27.8		-0.736

For the first three A-isomers (n = 0 - 2), the bond length change is negligible, and one would accordingly expect negligible charge donation as well. For the more electron-deficient A-isomers (n = 3 - 5), the bond length changes are a bit larger, but less than 10%, suggesting little charge donation.

For the B-isomers, on the other hand, the oxygen-oxygen bond length changes are predicted to be much larger (Tab. 4), about 30% corresponding to actual oxygen-oxygen bond lengths of roughly 1.3 Å. Based on the geometrical parameters of the $\rm O_2^-$ complexes, one may thus expect significant charge donation into the organic moiety in the Meisenheimer-like B-isomers.

A more direct indicator of the charge donation can be inferred from atomic charges computed with the NPA or MBIS atoms-in-molecules analysis schemes (see section 2). Either scheme produces almost identical results, and Tab. 4 lists the NPA-based charge of the " O_2^- " for the different $[O_2 \cdot C_6 H_{6-n} F_n]^-$ (n=3-6) anions. Before discussing the charge distribution, let us emphasize that only the negative charge, but not the spin population is impacted by complex formation. In other words,

the O_2 unit retains the entire unpaired spin, while it donates a certain percentage of its negative charge to the organic moiety. Thus, the $O_2^- \cdots$ fluorobenzene interaction is essentially mediated by a doubly occupied orbital.

The pattern reflects the trends in oxygen-oxygen bond lengths. In the first three A-isomers (n = 0 - 2), only 5 - 6% of the negative charge are donated onto the aromatic system, while the percentage is a bit higher (10 - 13%) for the second A-isomer group. The general increase with n is again clearly related to the increasing electron deficiency of the aromatic system, while the strong step-like increase from n = 2 to n = 3 is related to the change in O_2^- orientation (c.f. section 3.2).

In the light of their completely different binding motifs, it is hardly surprising that the B-isomers behave utterly differently. For n=3 and n=5, the nucleophilic O_2^- ion forms a strong dative bond with an electrophilic carbon atom in the sense that a significant part of the oxygen anion's negative charge (60%) are donated to the organic moiety. For n=6 charge donation is less dramatic: The O_2^- moiety donates only about 25% of its negative charge consistent with its considerably longer carbonoxygen bond length (see section 3.2). In other words, from a charge-donation perspective, $[O_2 \cdot C_6 F_6]^-$ is closer to the high-n A-isomers than to its B-isomer relations.

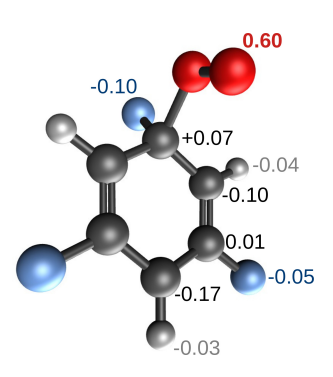


Figure 4: NPA charge changes Δq upon formation of the B-isomer of $[O_2 \cdot C_6 H_3 F_3]^-$. Charge changes are listed for the symmetry-unique atoms of the aromatic system and for the O_2 moiety.

Last, let us briefly examine where the donated change in the B-isomers localizes, and as a typical example, we consider $[O_2 \cdot C_6 H_3 F_3]^-$. Again, we don't present absolute NPA charges, but rather compute the change in NPA charge Δq upon complex formation:

$$O_2^- \ + \ C_6 H_3 F_3 \ \longrightarrow \ [O_2 \cdot C_6 H_3 F_3]^-.$$

For example, O_2^- has a charge of q=-1, while its charge in the B-isomer is about q=-0.4 (Tab. 4). Thus, the O_2 moiety donates 0.6 electron-charges, a Δq of +0.6. Note that accepting atoms show negative Δq values, and that the sum of charge changes must by definition vanish.

Figure 4 displays the charge changes for $[O_2 \cdot C_6 H_3 F_3]^-$. Strong increases of negative charge occur on the para-carbon (-0.17) as well as the ortho-carbons and the ipso-fluorine (-0.10). Much smaller negative Δq values can be observed for the meta-fluorine as well as the hydrogen atoms. The meta carbons show practically no charge change, and the only atom of the organic moiety showing a noticeable charge loss (+0.07)

is the ipso-carbon. All these charge changes follow naturally from the well-known resonance structures used to describe tight Meisenheimer complexes in organic chemistry: The negative charge is formerly delocalized over the ortho and para-carbons, while the hybridization of the ipso-carbon changes from sp_2 to sp_3 , causing the more polar ipso-CF bond. Thus, despite assuming fully formed nucleophile-carbon bonds and ignoring second-order effects such as inductive changes in the other CF and CH bonds, the Lewis structures of organic chemistry provide an excellent description of the charge changes upon $[\mathrm{O}_2\cdot\mathrm{C}_6H_3F_3]^-$ formation.

3.4. Charge-transfer anion excitations

In this section we consider complexes that can be thought of as neutral O_2 interacting with $C_6H_{6-n}F_n^-$ anions. Formerly, $O_2 \cdot C_6H_{6-n}F_n^-$ complexes represent charge-transfer (CT) excitations of the A or B isomers: one electron has been excited from O_2^- into the aromatic π -system. While photo-excitation of the anion ground states can only lead to spin doublet CT states, at least in principle, spin quartet CT states are also possible.

From a theoretical perspective, CT states of $[O_2 \cdot C_6 H_3 F_3]^$ anion complexes represent a far greater challenge than the associated ground states. In the first place, the relevant doublet states show multi-reference character. Both spin doublet and spin quartet CT states are best envisioned as a particular state of neutral oxygen coupled to a spin doublet of the anionic organic moiety. In this way, the high-spin component of the quartet CT state can be thought of as triplet oxygen coupled with the organic doublet. Similarly, the doublet CT state can be thought of as one of the oxygen singlet states coupling with the organic doublet. All configurations contributing to the two lowlying O₂ singlet states are involved—with different weights because the overall anion complex lacks symmetry and the O₂ π^* orbitals posses similar but non-identical energies. Hence, the quartet CT state is described with a single configuration and can be studied with standard single-reference methods. In contrast, the doublet CT state requires the inclusion of five configurations in the zeroth-order wavefunction (see supplementary information for a schematic representation of these configurations), and a multi-reference method such as the completeactive-space (CAS) self-consistent field (CASSCF) approach is needed. We note that standard excited-states methods, such as variants of EOM and ADC, yield for the spin doublet CT anions so-called spin-incomplete states because the five configurations needed as zeroth-order description are created as different excitation classes leading to an unbalanced treatment. In practical calculations, this can be seen by computing the \hat{s}^2 expectation value, which is expected to be 3/4, but shows values between 1.8 and 2.2.

In the second place, similar to the molecular anions $C_6H_{6-n}F_n^-$ (n=3-6) CT states of $[O_2\cdot C_6H_{6-n}F_n]^-$ represent electronically bound states only if their geometry is relaxed to the distorted ring structures of the organic moieties (see Figs. 1 and 2). In contrast, at the geometry of the A or B-anions or at the geometries of the corresponding neutral complexes, CT states do represent temporary anions. Any bound-state calculation at these structures yield negative vertical attachment

energies, which represent at best approximations for the resonance position, at worst, artifacts of the basis set (see discussion above).

In the third place, the distance and relative orientation of molecule-anion complexes in determined by a mixture of longrange and intermediate-range interactions. Any optimization method needs to account of these dynamic correlation effects either directly or indirectly.

Under these circumstances, it seems desirable to perform geometry optimizations with a suitably large CASSCF plus second-order perturbation scheme (CASPT2 or NEVPT2) taking dynamic correlation into account. To determine electron affinities, the geometry optimizations would then be followed by multi-reference configuration-interaction single-point energy evaluations, because electron affinities require methods approaching size extensivity.[43]

An alternative, less expensive, approximate, but still effective approach is the following: In a first step, the quartet states associated with the electron occupation of interest are optimized using the $\omega B97X$ -D3BJ DF and the def2-TZVPPD basis set. The quartet states represent high-spin single-reference states, and standard single-reference methods can be used for optimizations and single points. Specifically, the excitation energies of the quartet states relative to the anion ground states can be determined by performing single point CCSD(T) calculations with the aug-cc-pVTZ basis, since both states possess single reference character.

In a second step, multi-reference NEVPT2 single-point calculations with the aug-cc-pVTZ basis set are used to find the doublet-quartet splitting. In other words, the quartet states serve as a reference point to connect the energies of the ground state anions with that of the excited doublet CT states. The energies obtained with this less expensive scheme should be treated with appropriate caution: While all energy differences at the considered geometry can be considered reliable, the geometry of the doublet states is approximated by that of the quartet states. This difference is, however, expected to be small because the complex can be considered as a neutral triplet O_2 molecule attached to a anionic doublet fluorocarbon at a relatively large distance (see below). The difference between doublet and quartet states is therefore expected to be small.

Let us also note that in addition to providing a reference energy for connecting the ground and excited doublet states, the quartet states represent long-lived anion states of the system because they are vertically stable to electron detachment and their decay to the doublet ground state is spin forbidden. While quartet states are experimentally inaccessible by laser excitation from the ground state anions, they might be produced directly in the ion source of the experiment.

The geometrical structures of the quartet states are best described as loose clusters of O_2 molecules interacting with the π -system of a $C_6H_{6-n}F_n^-$ (n=3-6) anion. The lack of any short contacts indicating stronger interactions (C–O distances larger than 3.4 Å) can be explained by the properties of both moieties, which both tend to act as donors rather than as acceptors. Accordingly, at the minimal-energy structures of the quartet states, the doublet-quartet splittings are very small, and

Table 5: The first two columns list the AEA and adiabatic excitation energies E_X of the quartet states for $[O_2 \cdot C_6 H_{6-n} F_n]^-$ (n = 3 - 6) in eV; the third column lists the doublet-quartet splitting E_S in cm⁻¹. Both AEA and E_X have been evaluated with respect to the lowest energy isomer (A or B) of the respective neutral or anion. Zero-point corrections have not been applied. E_S is defined such that positive values indicate that the quartet state is more stable than the doublet.

acabict.			
n	AEA	E_X	E_S
3	-0.698	1.655	-66
4	-0.356	1.515	-3.4
5	0.071	1.158	3.7
6	0.278	0.697	12.9

at least at these geometries the doublet and quartet states are essentially isoenergetic.

Since the considered geometries represent loosely bound clusters of O_2 and $C_6H_{6-n}F_n^-$, the AEA essentially reflects that of the isolated $C_6H_{6-n}F_n$ molecules (note that in Tab. 1 zeropoint corrections of approximately 0.13 eV were applied, in contrast to the uncorrected values in Tab. 5). The presence of an oxygen molecule clearly has little impact on the electron binding energies of $C_6H_{6-n}F_n^-$ units, and the trends discussed in section 3.1 remain unchanged.

Provided the quartet geometries are reasonably close to those of the doublet states, we can draw the following conclusions regarding resonance contributions to the photoelectron spectra reported in Ref. [5]. On the one hand, the adiabatic excitation energies reported in Tab. 5 predict the onset of resonant excitation for each n. However, in going from the ground initial to the excited final state, the minimal energy geometry changes drastically, and one may thus expect a very broad Franck-Condon distribution. Moreover, in the vicinity of the vertical transition region, the final state corresponds to a short-lived temporary anion further broadening any resonance contribution to the overall signal.

4. Summary and Conclusions

This study aims to characterize the oxygen-fluorobenzene anion complexes, $[O_2 \cdot C_6 H_{6-n} F_n]^-$, that have recently been investigated by photodetachment spectroscopy.[5] We focus, in particular, on comparison of the complex with its constituting moieties: Changes in electron affinity upon complex formation and charge donation from the O_2^- anion to the organic ring system. Moreover, excited anion states corresponding to a neutral oxygen molecule bound to a fuorobenzene anion are briefly considered.

Both the vertical and adiabatic electron affinities of the $C_6H_{6-n}F_n$ molecules increase systematically with n. Still, all fluorobenzenes possess negative VEAs; in other words, at the neutral geometries, these organic molecules are unable to form stable valence states [C_6F_6 is known to form a non-valence anion state, see Ref. [44]], and adding an electron into the π^* LUMOs leads to the formation of short-lived temporary anions. Upon relaxation of the respective anions to their minimal energy geometries, local stability commences with n=3, that is, $C_6H_3F_3$ is the first member of the series showing a positive

VDE. Another two fluorine atoms are needed to achieve true stability: C_6HF_5 is the first fluorobenzene showing a positive AEA. However, even the AEA of C_6F_6 is smaller than that of O_2 , and it is thus natural to think of $[O_2 \cdot C_6H_{6-n}F_n]^-$ complexes as O_7^- bound to fluorobenzene units.

 $[ildo{O}_2 \cdot C_6 H_{6-n} F_n]^-$ complexes form two binding motifs, A-isomers that feature non-conventional hydrogen bonds, and Meisenheimer intermediate-like B-isomers that feature short O–C contacts. For both binding motifs, the inter-moiety interaction energy is substantial, $50-90\,\mathrm{kJ/mol}$, an order of magnitude larger than in the corresponding neutral clusters or in the associated CT states. Owing to the strong interaction, the O_2^- anion is stabilized, and the AEA of the complexes is significantly higher than that of the free O_2 molecule. For both isomers, the AEA generally increases strongly with the number of fluorine atoms, naturally following the electron deficiency of the organic moieties.

The strong $O_2^- \cdots C_6 H_{6-n} F_n$ interaction and short O–H or O– C distances indicate that the picture of an O₂ ion loosely attached to fluorobenzene units cannot be fully correct, and that the excess electron may not be localized entirely on the O₂ unit but rather delocalized to some extent over the entire complex (collectively-binding). The extent of charge donation to the organic moiety was characterized in two ways: The O-O bond length provides a proxy, since it will decrease with increasing charge donation, and the charge distribution in the complex anions can, of course, be directly compared to the charge distribution in the separate sub-units using atomic charges from various AIM analysis schemes. The following trends emerge: For the hydrogen-bonding motif (A-isomers), donation is moderate and grows with flurorination of the ring from about $0.05e^-$ for n = 0to $0.14e^-$ for n = 5. In contrast, the two tight Meisenheimer complexes (n = 3, 5) show substantial donation of more than half a charge (0.6e⁻), while the loose Meisenheimer complex formed by C₆F₆ falls between the other B-isomers and the high n A-isomers. Thus, the strong stabilization in the A-isomers can be characterized as primarily electrostatic in nature, while in the B-isomers a dative bond is formed delocalizing the negative charge. In other words, in A-isomers the excess electron can be characterized as essentially moiety-bound, while in Bisomers the excess electron shows collectively-bound character resembling, for example, electron binding in water cluster anions.

In addition to the ground states of the $[O_2 \cdot C_6 H_{6-n} F_n]^-$ complexes, we also characterized CT states corresponding to $O_2 \cdot C_6 H_{6-n} F_n^-$ complexes. Here, the neutral O_2 molecule is in its ground triplet state, which can spin-couple to the unpaired electron on the fluorobenzene anion to a total spin doublet or quartet state. Only the doublet states can be formed by laser excitation from the ground doublet states, however, at least in principle, the quartet state may be formed in the ion source.

The theoretical description of the excited doublet states requires multi-reference methods, and instead of directly optimizing the doublets, we were forced to use the energy of the quartets as points of reference: The theoretical description of the excited doublet anion states requires multi-reference methods, but we took advantage of the fact the associated single-

reference quartet states can be expected to very close in energy. Therefore, the energy difference between the CT quartet and the anion ground state can be determined from CCSD(T) because both states have single-reference character. On the other hand, owing to the multi-reference character of the doublet, a multi-reference method is needed to compute the energy difference between doublet and quartet, and we use CASSCF followed by NEVPT2 for this purpose. Moreover, similar to molecular fluorobenzene anions, CT $O_2 \cdot C_6 H_{6-n} F_n^-$ complexes are only electronically stable in the vicinity of their minimal energy geometries, and represent short-lived temporary anions otherwise.

Quartet $O_2 \cdot C_6 H_{6-n} F_n^-$ states show weak $O_2 \cdot \cdot \cdot C_6 H_{6-n} F_n^-$ interactions and much longer intermolecular distances than the A or B-isomers. Neutral O_2 is simply a bad acceptor, and the structures of the excited states resembles that of van der Waals clusters. Consequently, the structure of the organic moiety as such as well as its AEA is practically not impacted by the presence of the oxygen molecule. For the same reason the CT doublet and quartet states show only tiny splittings ($< 100 \, \text{cm}^{-1}$).

Based on these results, we predict that the resonance contribution to the photo-detachment spectrum will be very broad. On the one hand, at the geometries of the ground electronic states, the CT states are short-lived temporary anions. On the other hand, the equilibrium geometries of the anion ground and excited CT state differ strongly, both with regard to the interas with regard to the intramolecular coordinates, suggesting an extremely broad Franck-Condon envelope of electron energies.

Supplementary Material

See supplementary material for all optimized structures.

Acknowledgments

T.S. gratefully acknowledges stimulating discussions with Adrian Dempwolff as well as support from the National Science Foundation under Grant No. 2303652. C.C.J. gratefully acknowledges support from the National Science Foundation under Grant No. 2053889.

References

- [1] S. M. Ciborowski, G. Liu, J. D. Graham, A. M. Buytendyk, K. H. Bowen, Dipole-bound anions: Formed by Rydberg electron transfer (RET) and studied by velocity map imaging—anion photoelectron spectroscopy (VMI–aPES)., Eur. Phys. J. D 72 (2018) 139. doi:10.1140/epjd/e2018-90182-y.
- [2] E. F. Belogolova, G. Liu, E. P. Doronina, S. M. Ciborowski, V. F. Sidorkin, K. H. Bowen, Dipole-bound anions of intramolecular complexes, The Journal of Physical Chemistry Letters 9 (6) (2018) 1284–1289. doi:10.1021/acs.jpclett.8b00355.
- [3] V. F. Sidorkin, E. F. Belogolova, E. P. Doronina, G. Liu, S. M. Ciborowski, K. H. Bowen, "Outlaw" dipole-bound anions of intra-molecular complexes, Journal of the American Chemical Society 142 (4) (2020) 2001–2011. doi:10.1021/jacs.9b11694.
- [4] M. A. Dobulis, C. J. McGee, T. Sommerfeld, C. C. Jarrold, Autodetachment over broad photon energy ranges in the anion photoelectron spectra of [O₂–M]— (M = glyoxal, methylglyoxal, or biacetyl) complex anions, J. Phys. Chem. A 125 (2021) 9128.

- [5] M. Dobulis, M. Thompson, T. Sommerfeld, C. C. Jarrold, Temporary anion states of fluorine substituted benzenes probed by charge transfer in $O_2^- \cdot C_6 H_{6-x} F_x$ (x = 0 5) ion-molecule complexes., J. Chem. Phys. 152 (204309) 2020.
- [6] K. M. Ervin, I. Anusiewicz, P. Skurski, J. Simons, W. C. Lineberger, The only stable state of O₂⁻ is the X ²Π_g ground state and it (still!) has an adiabatic electron detachment energy of 0.45 ev, The Journal of Physical Chemistry A 107 (41) (2003) 8521–8529. doi:10.1021/jp0357323.
- [7] K. M. Patros, J. E. Mann, C. C. Jarrold, Photoelectron imaging spectra of O₂ ·VOC and O₄ ·VOC complexes, The Journal of Physical Chemistry A 120 (40) (2016) 7828–7838. doi:10.1021/acs.jpca.6b07107.
- [8] K. D. Jordan, P. D. Burrow, Studies of the temporary anion states of unstaturated hydrocarbons by electron transmission spectroscopy, Acc. Chem. Res. 11 (1978) 341–348.
- [9] J. K. Olthoff, J. A. Tossell, J. H. Moore, Electron attachment by haloalkenes and halobenzenes, The Journal of Chemical Physics 83 (11) (1985) 5627–5634. doi:10.1063/1.449687.
- [10] J. C. Giordan, J. H. Moore, J. A. Tossell, Anion states of paradisubstituted benzenes: 1,4-dihalobenzenes, Journal of the American Chemical Society 106 (24) (1984) 7397–7399. doi:10.1021/ja00336a017.
- [11] N. Driver, P. Jena, Electron affinity of modified benzene, International Journal of Quantum Chemistry 118 (4) (2018) e25504. doi:10.1002/qua.25504.
- [12] W. Koch, M. C. Holthausen, A chemist's guide to density functional theory, Wiley-VCH, 2000.
- [13] J. P. Perdew, K. Burke, M. Ernzerhof, Generalized gradient approximation made simple, Phys. Rev. Lett. 77 (1996) 3865.
- [14] H. Iikura, T. Tsuneda, T. Yanai, K. Hirao, A long-range correction scheme for generalized-gradient-approximation exchange functionals, The Journal of Chemical Physics 115 (8) (2001) 3540–3544. doi:10.1063/1.1383587.
- [15] A. P. Bartók, J. R. Yates, Regularized SCAN functional, The Journal of Chemical Physics 150 (16) (04 2019). doi:10.1063/1.5094646.
- [16] J. W. Furness, A. D. Kaplan, J. Ning, J. P. Perdew, J. Sun, Accurate and numerically efficient r2SCAN meta-generalized gradient approximation, The Journal of Physical Chemistry Letters 11 (19) (2020) 8208–8215. doi:10.1021/acs.jpclett.0c02405.
- [17] Y. Zhao, N. E. Schultz, D. G. Truhlar, Design of density functionals by combining the method of constraint satisfaction with parametrization for thermochemistry, thermochemical kinetics, and noncovalent interactions, Journal of Chemical Theory and Computation 2 (2) (2006) 364–382. doi:10.1021/ct0502763.
- [18] J.-D. Chai, M. Head-Gordon, Systematic optimization of long-range corrected hybrid density functionals, J. Chem. Phys. 128 (2008) 084106.
- [19] J.-D. Chai, M. Head-Gordon, Long-range corrected hybrid density functionals with damped atom-atom dispersion corrections, Phys. Chem. Chem. Phys. 10 (2008) 6615–6620. doi:10.1039/B810189B.
- [20] N. Mardirossian, M. Head-Gordon, ωB97X-V: A 10-parameter, range-separated hybrid, generalized gradient approximation density functional with nonlocal correlation, designed by a survival-of-the-fittest strategy, Phys. Chem. Chem. Phys. 16 (2014) 9904–9924. doi:10.1039/C3CP54374A.
- [21] A. Najibi, L. Goerigk, The nonlocal kernel in van der Waals density functionals as an additive correction: An extensive analysis with special emphasis on the B97M-V and ω B97M-V approaches, Journal of Chemical Theory and Computation 14 (11) (2018) 5725–5738. doi:10.1021/acs.jctc.8b00842.
- [22] A. Karton, A. Tarnopolsky, J.-F. Lamére, G. C. Schatz, J. M. L. Martin, Highly accurate first-principles benchmark data sets for the parametrization and validation of density functional and other approximate methods. derivation of a robust, generally applicable, double-hybrid functional for thermochemistry and thermochemical kinetics, The Journal of Physical Chemistry A 112 (50) (2008) 12868–12886. doi:10.1021/jp801805p.
- [23] D. Rappoport, F. Furche, Property-optimized gaussian basis sets for molecular response calculations, J. Chem. Phys. 133 (2010) 134105.
- [24] C. Riplinger, F. Neese, An efficient and near linear scaling pair natural orbital based local coupled cluster method, J. Chem. Phys. 138 (2013) 034106.
- [25] F. Neese, The ORCA program system, Wiley Interdisciplinary Reviews: Computational Molecular Science 2 (2012) 73–78.
- [26] F. Neese, F. Wennmohs, U. Becker, C. Riplinger, The orca quantum chem-

- istry program package, The Journal of Chemical Physics 152 (22) (2020) 224108.
- [27] N. Moiseyev, Quantum theory of resonances: Calculating energies, widths and cross-sections by complex scaling, Physics Reports 302 (1998) 211–293.
- [28] J. U. Davis Jr, T. Sommerfeld, Computing resonance energies directly: Method comparison for a model potential., Eur. Phys. J. D 75 (2021) 316.
- [29] T. Sommerfeld, R. J. Weber, Empirical correlation methods for temporary anions, J. Phys. Chem. A 115 (2011) 6675–6682.
- [30] J. Simons, Theoretical study of negative molecular ions, Ann. Rev. Phys. Chem. 62 (2011) 107–128.
- [31] J. Simons, Molecular anions perspective, The Journal of Physical Chemistry A 127 (18) (2023) 3940–3957. doi:10.1021/acs.jpca.3c01564.
- [32] J. C. Rienstra-Kiracofe, G. S. Tschumper, H. F. Schaefer III, S. Nandi, G. B. Ellison, Atomic and molecular electron affinities: Photoelectron experiments and theoretical computations, Chem. Rev. 102 (2002) 231.
- [33] T. H. Dunning Jr., Gaussian basis sets for use in correlated molecular calculations. I. the atoms boron through neon and hydrogen, J. Chem. Phys. 90 (1989) 1007–1023.
- [34] D. A. Matthews, J. F. Stanton, A new approach to approximate equationof-motion coupled cluster with triple excitations, J. Chem. Phys. 145 (2016) 124102.
- [35] D. A. Matthews, L. Cheng, M. E. Harding, F. Lipparini, S. Stopkowicz, T.-C. Jagau, P. G. Szalay, J. Gauss, J. F. Stanton, Coupled-cluster techniques for computational chemistry: The CFOUR program package, J. Chem. Phys. 152 (21) (2020) 214108.
- [36] J. Simons, Molecular anions, J. Phys. Chem. A 112 (2008) 6401.
- [37] A. E. Reed, R. B. Weinstock, F. Weinhold, Natural population analysis, J. Chem. Phys. 83 (1985) 735 – 746.
- [38] T. Verstraelen, S. Vandenbrande, F. Heidar-Zadeh, L. Vanduyfhuys, V. Van Speybroeck, M. Waroquier, P. W. Ayers, Minimal basis iterative stockholder: Atoms in molecules for force-field development, Journal of Chemical Theory and Computation 12 (8) (2016) 3894–3912. doi:10.1021/acs.jctc.6b00456.
- [39] D. G. A. Smith, L. A. Burns, A. C. Simmonett, R. M. Parrish, M. C. Schieber, R. Galvelis, P. Kraus, H. Kruse, R. Di Remigio, A. Alenaizan, A. M. James, S. Lehtola, J. P. Misiewicz, M. Scheurer, R. A. Shaw, J. B. Schriber, Y. Xie, Z. L. Glick, D. A. Sirianni, J. S. O'Brien, J. M. Waldrop, A. Kumar, E. G. Hohenstein, B. P. Pritchard, B. R. Brooks, H. F. Schaefer, A. Y. Sokolov, K. Patkowski, A. E. DePrince, U. Bozkaya, R. A. King, F. A. Evangelista, J. M. Turney, T. D. Crawford, C. D. Sherrill, Psi4 1.4: Open-source software for high-throughput quantum chemistry, The Journal of Chemical Physics 152 (18) (2020) 184108. doi:10.1063/5.0006002.
- [40] T.Y.Nikolaienko, L.A.Bulavin, D.M.Hovorun, JANPA: An open source cross-platform implementation of the natural population analysis on the Java platform, Computational and Theoretical Chemistry 1050 (2014) 15–22. doi:10.1016/j.comptc.2014.10.002.
- [41] Y. Gu, T. Kar, S. Scheiner, Fundamental properties of the CH···O interaction: Is it a true hydrogen bond?, Journal of the American Chemical Society 121 (40) (1999) 9411–9422. doi:10.1021/ja991795g.
- [42] IUPAC, Compendium of Chemical Terminology, 2nd Edition, Walter de Gryter, New York, 1997, (The Gold Book) Online corrected version: (2006 –). Meisenheimer complex. doi:10.1351/goldbook.M03819.
- [43] R. J. Bartlett, Many-body perturbation theory and coupled cluster theory for electron correlation in molecules, Annual Review of Physical Chemistry 32 (1981) 359–401.
- [44] V. K. Voora, K. D. Jordan, Nonvalence correlation-bound anion state of C₆F₆: Doorway to low-energy electron capture, The Journal of Physical Chemistry A 118 (35) (2014) 7201–7205. doi:10.1021/jp408386f.